Journal of Science and Technology in Civil Engineering NUCE 2020. 14 (1): 112–126

A CONSTANT FRICTION COEFFICIENT MODEL FOR CONCAVE FRICTION BEARINGS

Dao Dinh Nhan[a,*], Chung Bac Ai[a]

[a] *Civil Engineering Department, University of Architecture Ho Chi Minh City, 196 Pasteur Street, District 3, Ho Chi Minh City, Vietnam*

Article history:
Received 14/10/2019, Revised 05/12/2019, Accepted 06/12/2019

Abstract

This paper develops a constant friction coefficient model that best represents a velocity-dependent friction model for predicting structural response of buildings isolated with concave friction bearings. To achieve this goal, the effect of friction model on structural response of three hypothetical isolated buildings with different number of stories subjected to different earthquake scenarios was numerically investigated. The structural numerical models of the isolated buildings were developed in OpenSees with superstructure is represented by a shear frame model and isolation system using single friction pendulum bearings is modeled by a 3-D friction pendulum bearing element which accepts different friction models. The numerical models were subjected to 30 pairs of ground motions, representing service earthquake level, design basic earthquake level and maximum considered earthquake level at a strong seismic activity area in the world. The investigation reveals that friction coefficient models significantly affect the structural response and there is no constant friction coefficient model that simultaneously best predicts isolation system response and superstructure response. The constant friction coefficient that best predicts isolation system response produces a large error on prediction of superstructure response and vice versa. Based on the numerical results, a constant friction coefficient model for different criteria was developed.

Keywords: friction coefficient model; friction bearing; isolation system; earthquake response; time-history analysis.

https://doi.org/10.31814/stce.nuce2020-14(1)-10

1. Introduction

Concave friction bearings are among the most effective devices to protect buildings during earthquakes. This type of bearing consists of two outermost concave plates connected by intermediate slider(s) (Fig. 1). The sliding between sliders and concave plates provides flexibility to the bearing in horizontal directions and lengthens the horizontal vibrating period of the isolated structure therefore reduces the earthquake demand. Beside lengthening the vibrating period, sliding friction between sliders and the concave plates also provides damping to the system thus further reduces structural response. This effect is demonstrated in Fig. 2, which shows a typical design spectrum.

The parameters defining the behavior of a concave friction bearing are curvature of the sliding surfaces and friction coefficient between these surfaces. The curvature of the surfaces can be precisely determined from the geometry of the bearing. However, the friction coefficient between sliding

*Corresponding author. *E-mail address:* nhan.daodinh@uah.edu.vn (Nhan, D. D.)

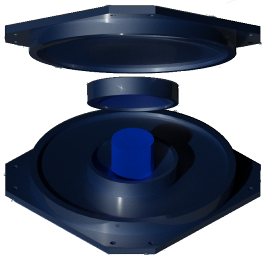

Figure 1. A concave friction bearing with multiple intermediate sliders

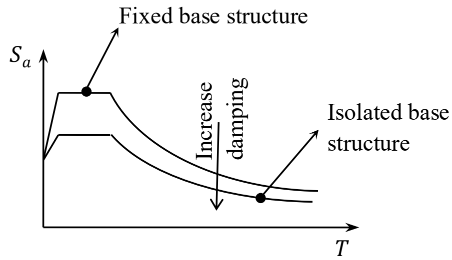

Figure 2. Typical design spectrum

surfaces is complicated. Past studies revealed that friction coefficient between surfaces is dependent on sliding velocity, contact pressure and temperature [1–3]. The dependence of friction coefficient on these parameters is schematically shown in Fig. 3. Among the parameters affecting friction coefficient, sliding velocity appears to have the most influence when the systems are subjected to earthquake ground motions. Because of that, many researchers employed the velocity-dependent friction coefficient model in their studies [4–7].

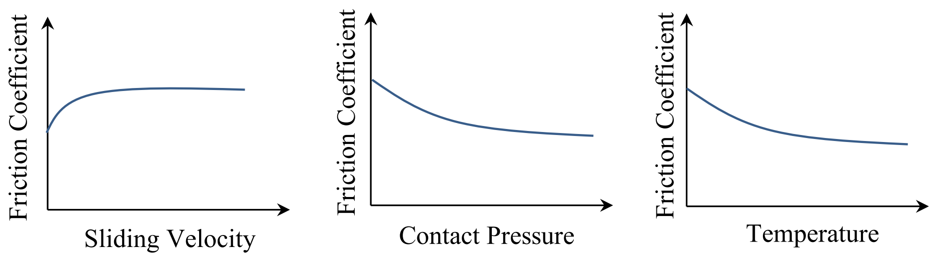

Figure 3. Dependency of friction coefficient on velocity, contact pressure and temperature

Although proper friction coefficient models are important to obtain reliable predicted response of an isolated building during earthquakes, many researchers used constant friction coefficient model for investigation [8–10] for its convenience. This simple friction model is also introduced to many design codes [11, 12]. Despite that the constant friction coefficient model is widely used both in research and design, few studies have ever investigated its validity and the instruction for selecting a proper friction coefficient for a certain purpose has not been recommended. This study aims to investigate the effect of constant friction model on the response of the computational models of three hypothetical buildings seismically isolated by single friction pendulum bearings subjected to different earthquake levels. Based on the investigation, constant friction models for different purposes shall be proposed.

2. Hysteresis loop of single friction bearings and friction coefficient model in consideration

Concave friction bearings in current practice can be single friction pendulum bearings or multiple friction pendulum bearings, depending on the number of pendulum mechanism they can produce. For investigating the effect of friction models on the response of the isolated buildings, this study only concentrates on single friction pendulum bearings.

The normalized unidirectional hysteresis loop, which shows the relationship between displacement and force, of a single friction pendulum bearing (Fig. 4(a)) with a constant friction model is presented in Fig. 4(b). In this figure, the horizontal axis represents displacement D of the bearing and the vertical axis represents the normalized force f, which is the ratio between the horizontal force F and the vertical force W in the bearing. R and μ are respectively radius and friction coefficient of the bearing as demonstrated in Fig. 4(a). The developing of this normalized hysteresis loop can be easily found in literature [13].

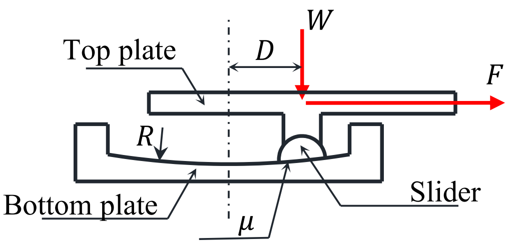

(a) Section view of the bearing

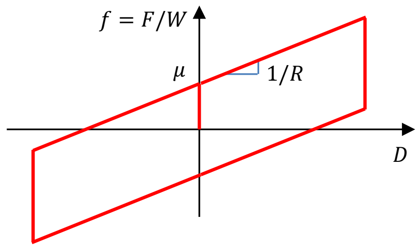

(b) Normalized hysteresis loop

Figure 4. Single friction pendulum bearing and its normalized hysteresis loop

If friction coefficient is not a constant, then the upper and lower bounds of the normalized hysteresis loop are not straight. The shape of the loop in this case is dependent on sliding velocity, contact pressure and temperature of the bearing. As explained earlier, effect of contact pressure and temperature on friction coefficient is neglected in this study. This assumption is consistent with many past studies [4–7]. The friction coefficient μ then can be expressed by Eq. (1) [14], which is widely used for friction bearings [2–7].

$$\mu = \mu_{fast} - \left(\mu_{fast} - \mu_{slow}\right) e^{-rv} \tag{1}$$

where μ_{fast} and μ_{slow} are friction coefficients at fast and slow velocities, respectively; v is sliding velocity; and r is a rate parameter.

Friction coefficients μ_{fast} and μ_{slow} depends on the vertical load and maximum load capacity of the bearing. From experimental data, [6] proposed that the ratio $\mu_{fast}/\mu_{slow} = 2.5$ can be used. Rate parameter r is a function of contact pressure and air temperature [1–3, 14]. This parameter for a certain friction model can be evaluated by assuming a reference sliding velocity and the correspondent reference friction coefficient. [6] used a reference sliding velocity $v_{ref} = 200$ mm/s, which is compatible with maximum sliding velocity expected during earthquakes, and reference friction coefficient $\mu_{ref} = 0.8\mu_{fast}$. These reference values are adopted in this investigation. Accordingly, r can be determined by Eq. (2).

$$r = \frac{1}{v_{ref}} \ln \frac{\mu_{fast} - \mu_{slow}}{\mu_{fast} - \mu_{ref}} = 0.0055 \text{ (s/mm)} \tag{2}$$

Given that the velocity-dependent friction coefficient model represented by Eq. (1) is widely accepted to account for the effect of sliding velocity on friction coefficient of friction pendulum bearings [2–7], this study considers it as the "exact" model for evaluating and optimizing constant friction models.

3. Numerical investigation

3.1. Hypothetical buildings and isolation systems

Three hypothetical buildings were selected for numerical investigation. These buildings are 5 bays by 5 bays in plan, with a span of 6 m for each bay. The number of stories of the investigated buildings were three, six and nine, with story height of 3.5 m. The selected number of stories are in the range where base isolation system is effective (i.e, between 1 to 10 stories as discussed by [14]). The seismic weight of 10 kN/m^2 were assumed for all buildings.

For investigation purpose, the structural system of the buildings was not designed in detail. Instead, their lateral stiffness was derived base on their assumed fundamental mode, which shall be presented in Section 3.2.

The buildings were assumed to locate in a strong seismic activity area of Los Angeles, California, USA with site class D (stiff-soil). From these data, short period spectral acceleration S_{as} and 1-s period spectral acceleration S_{a1} of the site at maximum consider earthquake (MCE) event and design basic earthquake (DBE) event were calculated per ASCE 7-16 [11] and presented in Table 1.

Table 1. Spectral acceleration at short period and 1 s-period for the site

	MCE event	DBE event
S_{as} (g)	2.432	1.622
S_{a1} (g)	1.279	0.853

Base isolation system for these buildings was designed according to the equivalent linear static procedure of ASCE 7-16 [11] such that its expected peak displacement in the DBE event is 30 cm and the 90-percentile-exceedance residual displacement is 5 cm. The residual displacement of the isolation system was estimated following [6]. To apply the equivalent linear static procedure, the constant friction coefficient model was used. This constant friction coefficient was taken as the reference friction coefficient described in Section 2.

Friction bearings with friction coefficient $\mu = 0.11$ and pendulum period $T_d = 4.8$ s (corresponding to a concave radius of $R = 5.73$ m) satisfy the design objectives and produce the smallest base shear coefficient, which is 0.162. This isolation system will generate an expected peak displacement of 61.4 cm and 90-percentile-exceedance residual displacement of 7 cm at MCE event. The expected base shear coefficient at MCE event is 0.217.

3.2. Computational model

Computational models of the isolated buildings were developed in OpenSees software [15]. The superstructure was modelled as a bidirectional shear frame structure whose story stiffness was computed from the fundamental mode of the fixed base configuration following a procedure developed in [16]. This type of superstructure model has been widely used in past studies of isolated buildings [17–22]. The mode shapes of the fundamental modes in both horizontal directions are assumed to be linear distribution with respect to height. The fundamental periods T_1 of the structures were predicted from Eq. (3), which conforms to [23].

$$T_1 = 0.15\,\mathrm{N} \tag{3}$$

where N is number of stories of the building.

Story stiffness and seismic mass of the computational models are presented in Table 2. The seismic mass of the models was computed from the floor area (which is 30 m by 30 m) and seismic weight of 10 kN/m^2 as mentioned earlier. Note that the weight of base, which is twice of typical floor weight, was included in the model but not listed in the table.

The buildings are expected to be damage-free during considered earthquakes, which is reasonable for isolated buildings, such that the superstructures are assumed to possess linear behavior. This assumption is widely used in research.

In computational modelling technique, a bidirectional shear frame structure can be modelled as a stick model where a floor is lumped into one node. This node carries the whole mass of the floor.

Table 2. Story stiffness and floor mass of the buildings

	Stiffness (MN/m)			Mass (tons)		
	3-story building	6-story building	9-story building	3-story building	6-story building	9-story building
Story 1	1053	3685	7896	900	900	900
Story 2	877	3509	7720	900	900	900
Story 3	526	3158	7369	900	900	900
Story 4	-	2632	6843	-	900	900
Story 5	-	1930	6141	-	900	900
Story 6	-	1053	5264	-	900	900
Story 7	-	-	4211	-	-	900
Story 8	-	-	2983	-	-	900
Story 9	-	-	1579	-	-	900

Rotational degree of freedom of these nodes are restrained. The two adjacent nodes (representing the two adjacent floors) are connected by a bidirectional shear spring whose stiffness equals the shear stiffness of the story.

The bearings in the isolation system were lumped to the center of the base and modeled by a triple friction pendulum bearing element [24]. This element can be used to model friction bearings with single, double and triple pendulum mechanisms. This study uses the element to model the single friction pendulum bearings. Both constant friction model and velocity dependent friction model were used to investigate the effect of friction model on the response of the isolated buildings. Rate parameters of velocity-dependent friction model were determined from Eq. (2).

Energy dissipated mechanism in the computational model was captured through Rayleigh damping model [25] calibrated to 1.0 percentage of critical viscous damping at 4.8 s period and T_2 period. 4.8 s is the pendulum period of the isolation system and T_2 is the period of the second mode of the isolated configuration, which depends on the buildings and are computed through an eigen analysis of the isolated model. Effective period of 2.72 s for the isolation system, which is correspondent to the target peak displacement of 30 cm at DBE event, mentioned earlier, was used for the eigen analysis.

3.3. Input ground motions

This study employs the ground motions from [26] as the input for dynamic analysis of the isolated models. Accordingly, three sets of ground motions representing MCE event, DBE event and service earthquake (SE) event of the site, i.e. Los Angles city and site class D, were proposed. Each set contains ten pairs of ground motion. Each pair consists of two horizontal components of the ground shaking. Detail information of the selected motion is presented in [26]. It is noted that five in ten ground motions for MCE event are simulated motions. For the purpose of this study, only two of the simulated motions was used. Thus, the number of seven ground motions for MCE event was adopted. This number of ground motions is sufficient for using average value to evaluate response of structures, as required by [11]. Fig. 5 shows the square-root-of-sum-square (SRSS) of the pseudo acceleration spectra of individual motions along with the average spectrum over all motions for the three events.

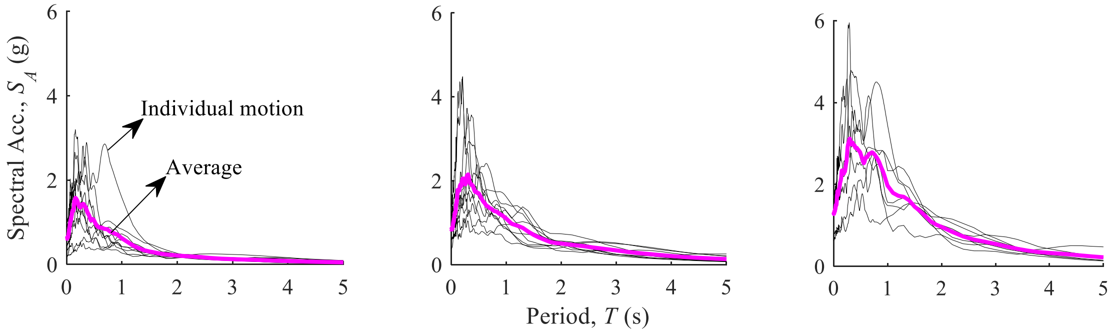

(a) SE event (b) DBE event (c) MCE event

Figure 5. Spectral acceleration of selected ground motions

3.4. Results and discussions

Nonlinear time-history dynamic response of the numerical models to the selected ground motions was analyzed using Newmark method in combination with Newton-Raphson iteration. Fig. 6 shows the hysteresis loop of the isolation system in the fault-parallel direction of the 6-story model subjected to a ground motion recorded from 1994 Northridge earthquake. This motion is among the seven motions representing MCE earthquakes. Both hysteresis loops for the model using isolation system with general friction model (Gen. Fric.) and the model using isolation system with reference friction model (Ref. Fric.) are presented in this figure. It can be observed that the peak displacements of the two models are similar but the hysteresis loops are significantly different. Hysteresis loop for Gen. Fric. is smoother, i.e. the change of the base shear is smoother, than the hysteresis loop for Ref. Fric. at reversal movements. This comes from the fact that friction coefficient gradually decreases with the decreasing of sliding velocity in Gen. Fric., while maintains a constant value in Ref. Fric. Note that the hysteresis loop for Ref. Fric. is much smoother than expected due to the bi-directional movement effect.

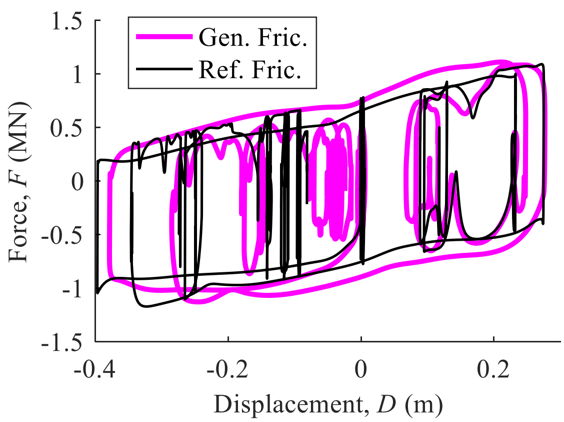

Figure 6. Hysteresis loop of the isolation system in the 6-story building

The difference in friction model also affects the superstructure response as shown in Fig. 7, which presents the acceleration history during the first 10 seconds at roof in the considered direction. Peak acceleration in Ref. Fric. is much larger than that in Gen. Fric. although the peak displacements in the two models are similar as mentioned. This comes from the sudden change in the base shear at reversal movements in Ref. Fric. as explained earlier.

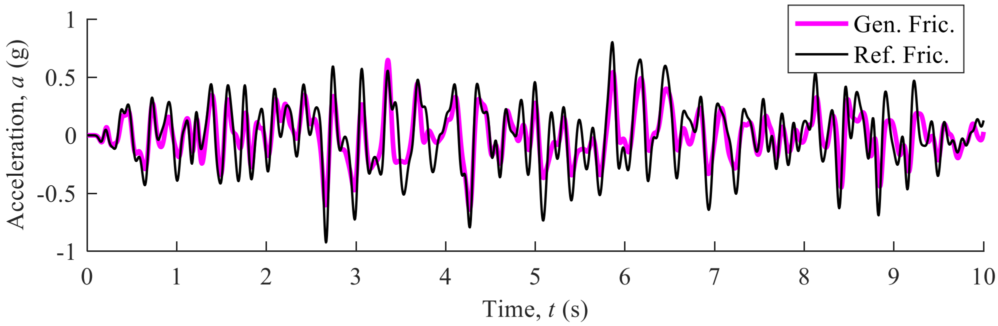

Figure 7. Floor acceleration at roof of the 6-story building

To further investigate the effect of friction model on the structural response, average of the peak response was computed for comparison. The average of the peak response for an earthquake event, R, is evaluated as:

$$R = \frac{1}{N}\sum_{i=1}^{N} R_i \tag{4}$$

where R_i is the peak response subjected to ground motion i in an earthquake event and N is the number of ground motions in the event.

Fig. 8 presents the average of peak displacement of isolation system, $D_{\max}$, for all computational models in all earthquake events. The figure shows that $D_{\max}$ generated by Gen. Fric. model and Ref. Fric. model are comparable. This result indicates that Ref. Fric. model is a good representation of Gen. Fric. model in predicting average peak displacement of the isolation system.

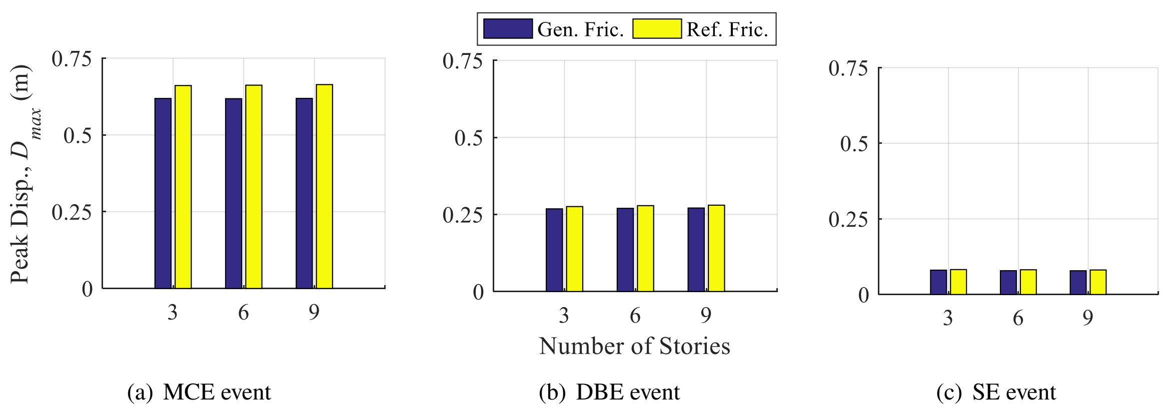

Figure 8. Average of peak displacement of isolation system

Fig. 9 shows the average of peak story drift $d_{\max}$, which is the ratio between relative displacement of adjacent floors of a story and story height, of the investigated models at different earthquake events. The result shows significant difference between the friction models. This large difference can also be observed in the average of peak floor acceleration $a_{\max}$ (Fig. 10).

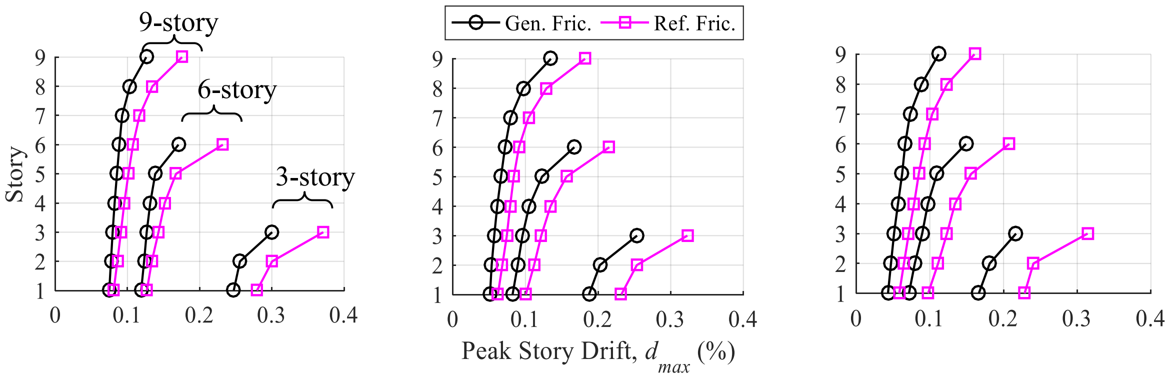

(a) MCE event (b) DBE event (c) SE event

Figure 9. Average of peak story drift

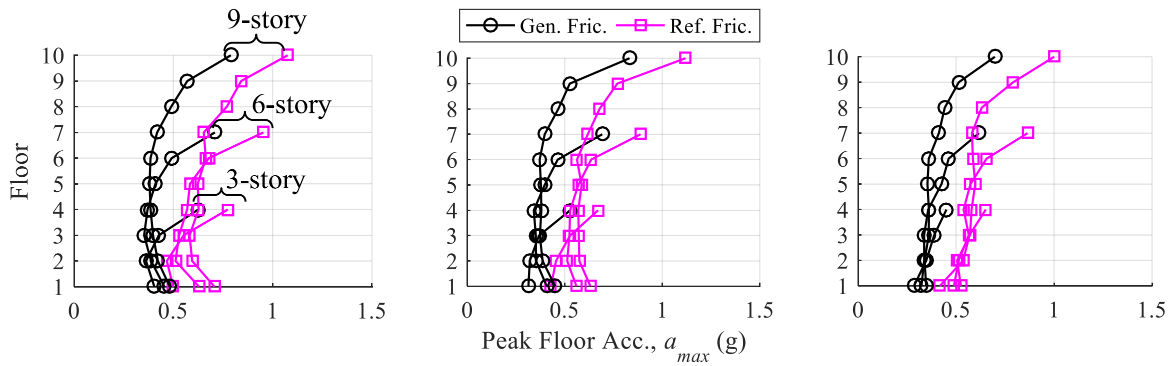

(a) MCE event (b) DBE event (c) SE event

Figure 10. Average of peak floor acceleration

To quantify the difference between the responses of the computational models with Gen. Fric. and Ref. Fric., the average error E_{mD}, E_{md} and E_{ma} of the averages of the peak displacement of isolation system, peak story drift and peak floor acceleration defined by Eqs. (5)–(7) was evaluated. Note that these errors are computed for individual computational model at each earthquake level.

$$E_{mD} = \left| \frac{D_{\max,Ref} - D_{\max,Gen}}{D_{\max,Gen}} \right| \tag{5}$$

$$E_{md} = \frac{1}{N_{st}} \sum_{i=1}^{N_{st}} \left| \frac{d_{\max,i,Ref} - d_{\max,i,Gen}}{d_{\max,i,Gen}} \right| \tag{6}$$

$$E_{ma} = \frac{1}{N_{fl}} \sum_{i=1}^{N_{fl}} \left| \frac{a_{\max,i,Ref} - a_{\max,i,Gen}}{a_{\max,i,Gen}} \right| \tag{7}$$

where $D_{\max,\,Ref}$ and $D_{\max,\,Gen}$ are the average of the peak displacement of isolation system of the computational models using Ref. Fric. and Gen. Fric., respectively; $d_{\max,i,Ref}$ is the average of peak story drift at story i of the computational model using Ref. Fric.; $d_{\max,i,Gen}$ is the average of peak story drift at story i of the computational model using Gen. Fric; $a_{\max,i,Ref}$ is the average of peak floor acceleration at floor i of the computational model using Ref. Fric.; $a_{\max,i,Gen}$ is the average of peak floor acceleration at floor i of the computational model using Gen. Fric; N_{st} is the number of stories; and N_{fl} is the number of floors.

The average errors E_{mD}, E_{md} and E_{ma} are plotted in Figs. 11(a), 11(b) and 11(c), respectively. The results in these figures shows that the numerical model using Ref. Fric. can capture the peak displacement of the isolation system of the computational model using Gen. Fric. well, with the error of less than 10%. However, the error is quite large for peak story drift and peak floor acceleration, with the error can be larger than 50% for peak floor acceleration response. This observation suggests that the Ref. Fric. model is not good for predicting story drift and floor acceleration.

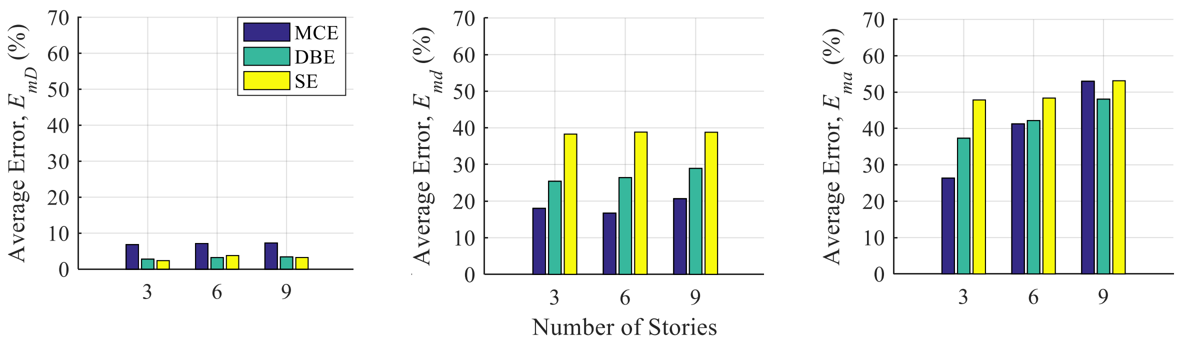

(a) Displacement of isolation system

(b) Story drift

(c) Floor acceleration

Figure 11. Average error of predicted responses of models using reference friction coefficient

To derive an optimal constant friction model that can be used to best predict the response of computational model using Gen. Fric. model, normalized errors E_{nD}, E_{nd} and E_{na} of the averages of peak displacement of isolation system, peak story drift and peak floor acceleration are defined by Eqs. (8)–(10). Similar to the average errors, the normalized errors were also computed for individual computational model in an earthquake event.

$$E_{nD} = \left| \frac{D_{\max,Ref} - D_{\max,Gen}}{D_{\max,Gen}} \right| \tag{8}$$

$$E_{nd} = \frac{1}{N_{st}} \sqrt{\sum_{i=1}^{N_{st}} \left(\frac{d_{\max,i,Ref} - d_{\max,i,Gen}}{d_{\max,i,Gen}} \right)^2} \tag{9}$$

$$E_{na} = \frac{1}{N_{fl}} \sqrt{\sum_{i=1}^{N_{fl}} \left(\frac{a_{\max,i,Ref} - a_{\max,i,Gen}}{a_{\max,i,Gen}} \right)^2} \tag{10}$$

The optimal constant friction coefficient will minimize these normalized errors. Note that the average errors defined by Eqs. (5)–(7) are used to evaluate the average errors of the computational model using constant friction coefficient whereas the normalized errors defined by Eqs. (8)–(10), which consider not only the average error but also the dispersion of the error, are used as objective functions to find the optimal constant friction coefficient. This approach is common in practice.

For convenience, a normalized friction coefficient c_n correspondent to a constant friction coefficient $\hat{\mu}$ is defined as:

$$c_n = \frac{\hat{\mu} - \mu_{slow}}{\mu_{fast} - \mu_{slow}} \tag{11}$$

The optimal constant friction coefficient, μ_{opt}, is expected to be in the range of (μ_{slow}, μ_{fast}) so that only $\mu_{slow} \leq \hat{\mu} \leq \mu_{fast}$ is considered. In that range, c_n is bounded between 0 and 1 and is linearly dependent on $\hat{\mu}$. The c_n corresponding to μ_{opt} hereafter is referred to as optimal normalized friction coefficient c_{opt}. Depending on the type of response in consideration (i.e. displacement of isolation system, story drift and floor acceleration), the subscript of "D", "d" and "a", respectively, will be added to c_{opt} (and thus μ_{opt}).

The variation of E_{nD} for the investigated buildings at different earthquake event on c_n are plotted in Fig. 12. The figure shows that $c_{opt,D}$, which minimize E_{nD}, is slightly dependent on building models and earthquake event. These optimal values are presented in Table 3. The results show that Gen. Fric., which use $\mu = 0.8\mu_{fast}$, produces a $c_n = 0.667$, which is slightly smaller than $c_{opt,D}$ for all building at all earthquake events.

Table 3. Optimal normalized friction coefficient for peak displacement of isolation system

Building	Earthquake events		
	MCE	DBE	SE
3-story	0.85	0.70	0.95
6-story	0.85	0.75	0.90
9-story	0.85	0.75	0.80

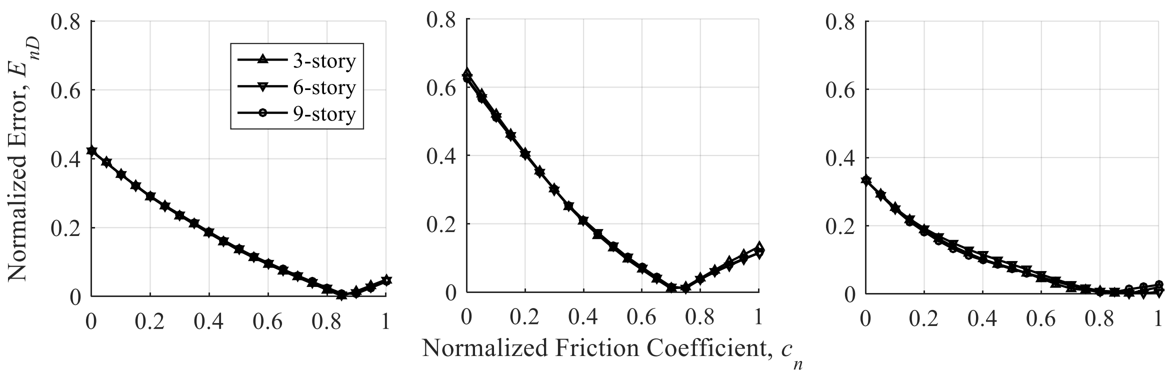

(a) MCE event (b) DBE event (c) SE event

Figure 12. Normalized error of peak displacement of isolation system

The variation of E_{nd} and E_{na} on c_n is plotted in Figs. 13 and 14. The optimal normalized friction coefficient is presented in Tables 4 and 5. These results show that the optimal constant friction coef-

Table 4. Optimal normalized friction coefficient for peak story drift

Building	Earthquake events		
	MCE	DBE	SE
3-story	0.40	0.35	0.20
6-story	0.40	0.25	0.20
9-story	0.35	0.30	0.15

Table 5. Optimal normalized friction coefficient for peak floor acceleration

Building	Earthquake events		
	MCE	DBE	SE
3-story	0.35	0.25	0.15
6-story	0.20	0.10	0.05
9-story	0.10	0.15	0.05

ficient depends on not only the type of response in consideration, but also the building model as well as earthquake event. There is no constant friction coefficient that minimizes all normalized errors.

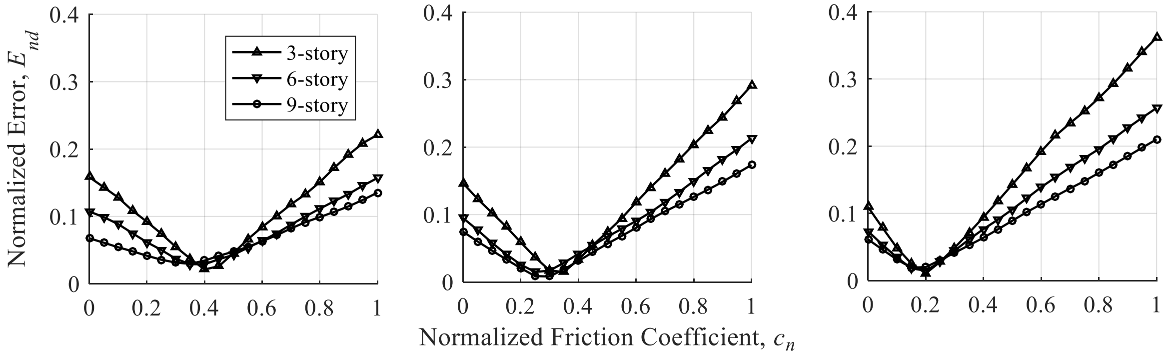

(a) MCE event (b) DBE event (c) SE event

Figure 13. Normalized error of peak story drift

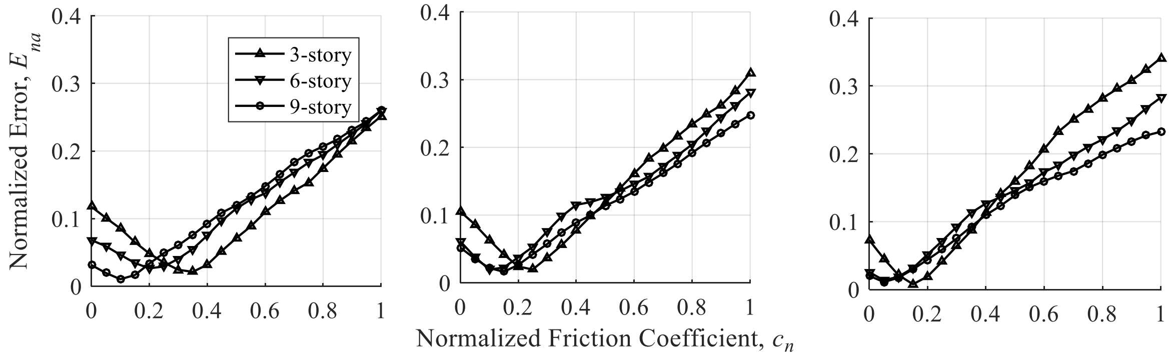

(a) MCE event (b) DBE event (c) SE event

Figure 14. Normalized error of peak floor acceleration

To develop a "best-fit" constant friction coefficient model that takes all responses in to consideration, a combined normalized error function E_t is defined as:

$$E_t = \sum_{Event} \sum_{Model} w_D E_{nD} + \sum_{Event} \sum_{Model} w_d E_{nd} + \sum_{Event} \sum_{Model} w_a E_{na} \tag{12}$$

where w_D, w_d and w_a are weighting factors for E_{nD}, E_{nd} and E_{na}, respectively, which satisfy Eq. (13):

$$\sum_{Event} \sum_{Model} w_D + \sum_{Event} \sum_{Model} w_d + \sum_{Event} \sum_{Model} w_a = 1 \tag{13}$$

Assume that $w_a = w_d = w_s$, i.e. story drift and floor acceleration take the same important order. Assume also that all building models and all earthquake events are equal in optimization, Eq. (12)

becomes:

$$E_t = w_D \sum_{Event} \sum_{Model} E_{nD} + w_s \left(\sum_{Event} \sum_{Model} E_{nd} + \sum_{Event} \sum_{Model} E_{na} \right) \tag{14}$$

For each ratio of w_s/w_D, the combined normalized error E_t at different normalized friction coefficient c_n can be determined. From the variation of E_t on c_n, the optimal c_{opt} can be identified. This is the optimal normalized friction coefficient corresponding to a certain value of w_s/w_D. Different w_s/w_D produces different c_{opt}. The dependency of c_{opt} on w_s/w_D is shown in Fig. 15. The figure suggests that optimal normalized friction coefficient for analyzing peak displacement of isolation system ($w_s/w_D = 0$) is $c_n \simeq 0.8$. The optimal normalized friction coefficient for analyzing peak structural response, including story drift and floor acceleration, ($w_s/w_D \to \infty$) is $c_n \simeq 0.2$. Table 6 summarizes the optimal normalized friction coefficient and correspondent constant friction coefficient for special cases.

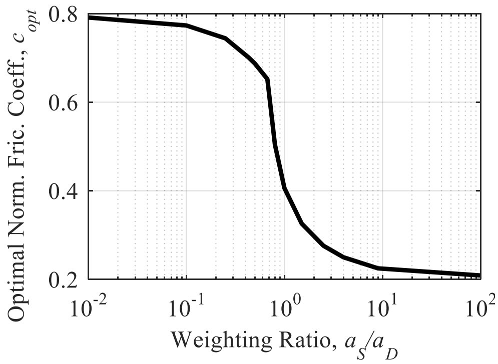

Figure 15. Optimal normalized friction coefficient

Table 6. Optimal constant friction coefficient for different criteria

Criteria	c_{opt}	μ_{opt}
Best predict displacement of isolation system ($a_s/a_D = 0$)	0.8	$0.88\mu_{fast}$
Best predict structural response ($a_s/a_D \to \infty$)	0.2	$0.52\mu_{fast}$
Best predict overall response ($a_s/a_D = 2$)	0.3	$0.58\mu_{fast}$

Fig. 16 shows average error of the predicted peak responses for the numerical model using friction model for best predicting displacement of isolation system (i.e. $\mu = 0.88\mu_{fast}$). The figure shows that the average error of the peak displacement is smaller than 5%. However, the prediction of story drift and floor acceleration is low accurate, with the average error goes up to about 50% and 60% for story drift and floor acceleration, respectively.

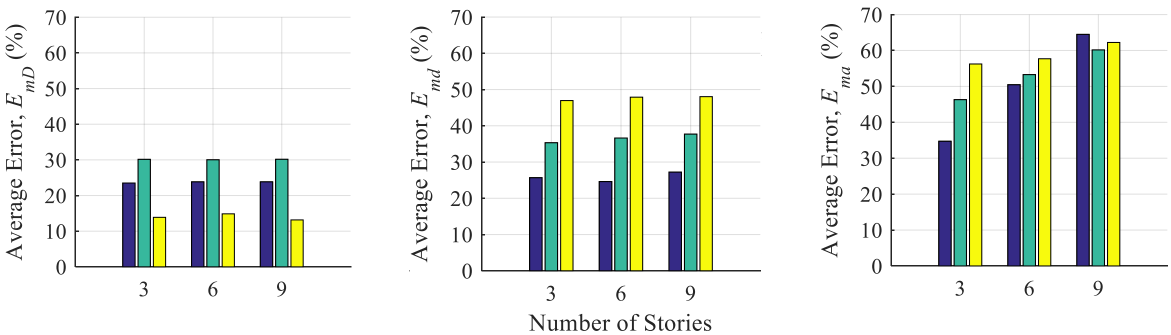

(a) Displacement of isolation system (b) Story drift (c) Floor acceleration

Figure 16. Average error of predicted responses of models using best isolation system response friction coefficient

The average error for predicted response of the numerical model using the constant friction model that best predicts structural responses is plotted in Fig. 17. The result shows that the average error of story drift and floor acceleration is low, but the average error of predicted isolation system's displacement is high, with the average error can be up to 40%.

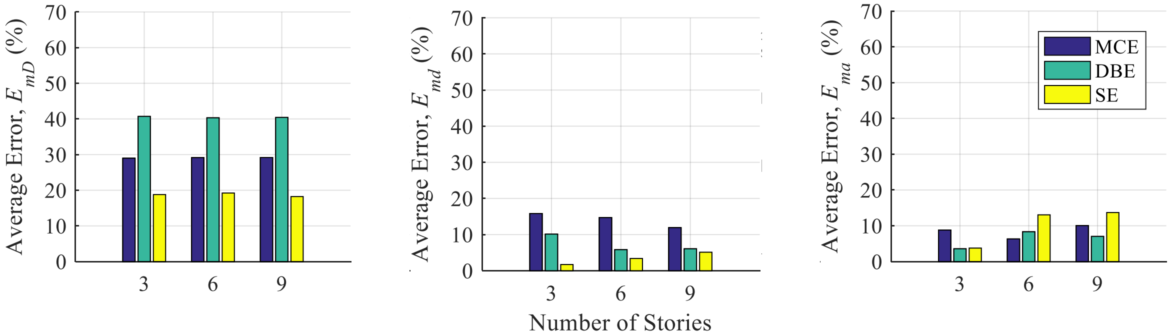

(a) Displacement of isolation system (b) Story drift (c) Floor acceleration

Figure 17. Average error of predicted responses of models using best superstructure response friction coefficient

The comparison between results in Figs. 16 and 17 shows that peak displacement of the isolation system is easier to predict than the peak story drift or peak floor acceleration. The largest error of the best predicted isolation system's displacement is less than 5% while the largest error of the best predicted story drift and floor acceleration is around 15%.

Fig. 18 shows the average error of the predicted response of the numerical model using constant friction model that best predicts overall response. The error is less than 30% for all response of all models. The error for peak story drift, which is smaller than 15%, is the smallest.

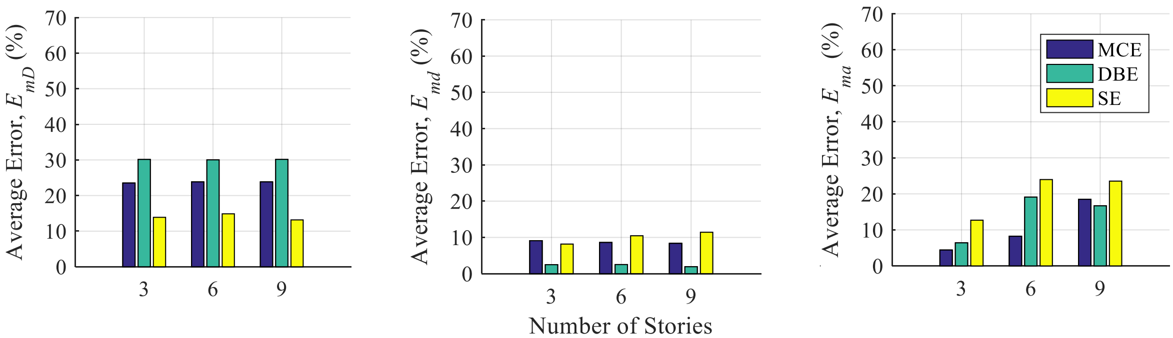

(a) Displacement of isolation system (b) Story drift (c) Floor acceleration

Figure 18. Average error of predicted responses of models using best overall response friction coefficient

4. Conclusions

The investigation of the responses of the numerical models of three-, six- and nine-story buildings isolated by single friction pendulum bearings subjected to different earthquake levels in this paper shows that friction model strongly affects the response of the isolated buildings and there is no best constant friction model that can simultaneously minimize the error of all predicted responses. The constant friction model that produces the best prediction of peak displacement of isolation systems generates very large error on predicted peak story drift and peak floor acceleration. Likewise, the constant friction model that best predicts peak story drift and peak floor acceleration cannot accurately predict peak displacement of isolation system. The investigation shows that the constant friction model with $\mu = 0.88\mu_{fast}$ best predicts the peak displacement of isolation systems, the constant friction model with $\mu = 0.52\mu_{fast}$ best predicts peak story drift and peak floor acceleration. For predicting overall responses, including isolation system's displacement, story drift and floor acceleration, the constant friction model with $\mu = 0.58\mu_{fast}$ should be used. The best constant friction model corresponding to different criteria are given in Fig. 15. These best-fit constant friction coefficients were derived base on common value of parameters defining velocity-dependent friction coefficient model. Further investigation may be needed to derive a more general result.

Acknowledgement

This research is funded by Vietnam National Foundation for Science and Technology Development (NAFOSTED) under grant number 107.01-2017.21. The authors are grateful for this financial support.

References

[1] Mokha, A., Constantinou, M., Reinhorn, A. (1990). Teflon bearings in base isolation I: Testing. *Journal of Structural Engineering*, 116(2):438–454.

[2] Dolce, M., Cardone, D., Croatto, F. (2005). Frictional behavior of steel-PTFE interfaces for seismic isolation. *Bulletin of Earthquake Engineering*, 3(1):75–99.

[3] Quaglini, V., Dubini, P., Poggi, C. (2012). Experimental assessment of sliding materials for seismic isolation systems. *Bulletin of Earthquake Engineering*, 10(2):717–740.

[4] Fenz, D. M., Constantinou, M. C. (2008). Modeling triple friction pendulum bearings for response-history analysis. *Earthquake Spectra*, 24(4):1011–1028.

[5] Rabiei, M., Khoshnoudian, F. (2011). Response of multistory friction pendulum base-isolated buildings including the vertical component of earthquakes. *Canadian Journal of Civil Engineering*, 38(10):1045–1059.

[6] Cardone, D., Gesualdi, G., Brancato, P. (2015). Restoring capability of friction pendulum seismic isolation systems. *Bulletin of Earthquake Engineering*, 13(8):2449–2480.

[7] Ponzo, F. C., Di Cesare, A., Leccese, G., Nigro, D. (2017). Shake table testing on restoring capability of double concave friction pendulum seismic isolation systems. *Earthquake Engineering & Structural Dynamics*, 46(14):2337–2353.

[8] van de Lindt, J. W., Jiang, Y. (2013). Empirical selection equation for friction pendulum seismic isolation bearings applied to multistory woodframe buildings. *Practice Periodical on Structural Design and Construction*, 19(3):1–10.

[9] Peng, P., Dongbin, Z., Yi, Z., Yachun, T., Xin, N. (2018). Development of a tunable friction pendulum system for semi-active control of building structures under earthquake ground motions. *Earthquake Engineering & Structural Dynamics*, 47(8):1706–1721.

[10] Xu, Y., Guo, T., Yan, P. (2019). Design optimization of triple friction pendulums for base-isolated high-rise buildings. *Advances in Structural Engineering*, 22(13):2727–2740.

[11] ASCE 7-16 (2017). *Minimum design loads and associated criteria for buildings and other structures*. ASCE/SEI 7-16.

[12] Eurocode 8 (2004). *Design of structures for earthquake resistance*. European Committee for Standardization.

[13] Morgan, T. A. (2011). The use of innovative base isolation systems to achieve complex seismic performance objectives. Technical report, Report No. PEER-2011/06, Pacific Earthquake Engineering Research Center, University of California, Berkeley.

[14] Constantinou, M., Mokha, A., Reinhorn, A. (1990). Teflon bearings in base isolation II: Modeling. *Journal of Structural Engineering*, 116(2):455–474.

[15] McKenna, F. (1997). *Open source for earthquake engineering simulation*. UC Berkeley.

[16] Dao, N. D., Ryan, K. L., Nguyen-Van, H. (2019). Evaluating simplified models in predicting global seismic responses of a shake table–test building isolated by triple friction pendulum bearings. *Earthquake Engineering & Structural Dynamics*, 48(6):594–610.

[17] Jangid, R. S. (1996). Seismic response of an asymmetric base isolated structure. *Computers & Structures*, 60(2):261–267.

[18] Jangid, R. S. (2000). Seismic response of structures with sliding systems. *Journal of Seismology and Earthquake Engineering*, 2(2):45–54.

[19] Lee, D.-G., Hong, J.-M., Kim, J. (2001). Vertical distribution of equivalent static loads for base isolated building structures. *Engineering Structures*, 23(10):1293–1306.

[20] Wang, J. Q., Ding, Y. G., Li, D. W. (2011). Seismic response of the asymmetric structure isolated by the friction sliding bearings. *Advanced Materials Research*, 163:4218–4221.

[21] Fallahian, M., Khoshnoudian, F., Loghman, V. (2015). Torsionally seismic behavior of triple concave friction pendulum bearing. *Advances in Structural Engineering*, 18(12):2151–2166.

[22] Thanh, N. X. (2017). Nonlinear dynamic analysis of base-isolated frames using Julia. *Journal of Science and Technology in Civil Engineering (STCE)-NUCE*, 11(6):29–36.

[23] Naqash, M. T. (2014). Study on the fundamental period of vibration of steel moment resisting frames. *International Journal of Advanced Structures and Geotechnical Engineering*, 3(01):01–06.

[24] Dao, N. D., Ryan, K. L., Sato, E., Sasaki, T. (2013). Predicting the displacement of triple pendulum™ bearings in a full-scale shaking experiment using a three-dimensional element. *Earthquake Engineering & Structural Dynamics*, 42(11):1677–1695.

[25] Chopra, A. K. (2015). *Dynamics of structures: theory and applications to earthquake engineering*. Prentice Hall, Upper Saddle River, NJ, USA.

[26] Somerville, P., Smith, N. F., Punyamurthula, S., Sun, J. I. (1997). *Development of ground motion time histories for phase 2 of the FEMA/SAC steel project*. FEMA report.